Leung, Yee; Ge, Yong; Ma, Jianghong; Wang, Jinfeng

Conference Paper

Measurement Errors and their Propagation in the Registration of Remote Sensing Images

43rd Congress of the European Regional Science Association: "Peripheries, Centres, and Spatial Development in the New Europe", 27th - 30th August 2003, Jyväskylä, Finland

Provided in Cooperation with:
European Regional Science Association (ERSA)

Measurement Errors and their Propagation in the Registration of Remote Sensing Images

Yee Leung[1], Yong Ge[2, 4], Jianghong Ma[3], Jinfeng Wang[2]

1. Department of Geography and Resource Management, The Chinese University of Hong Kong, Shatin, Hong Kong.
   E-mail: yeeleung@cuhk.edu.hk

2. State Key Laboratory of Resources and Environmental Information System, Institute of Geographic Sciences & Natural Resources Research, Chinese Academy of Sciences, Beijing 100101, China

3. Institute for Information and System Science, Faculty of Science, Xi' an Jiaotong University, Xi' an 710049, China

4. Laboratory of Remote Sensing Information Sciences, Institute of Remote Sensing Applications, CAS, Beijing 100101, China.

Abstract

Reference control points (RCPs) used in establishing the regression model in the registration or geometric correction of remote sensing images are generally assumed to be "perfect". That is, the RCPs, as explanatory variables in the regression equation, are accurate and the coordinates of their locations have no errors. Thus ordinary least squares (OLS) estimator has been applied extensively to the registration or geometric correction of remotely sensed data. However, this assumption is often invalid in practice because RCPs always contain errors. Moreover, the errors are actually one of the main sources which lower the accuracy of geometric correction of an uncorrected image. Under this situation, the OLS estimator is biased. It cannot handle explanatory variables with errors and cannot propagate appropriately errors from the RCPs to the corrected image. Therefore, it is essential to develop new feasible methods to overcome such a problem.

In this paper, we introduce the consistent adjusted least squares (CALS) estimator and propose a relaxed consistent adjusted least squares (RCALS) method, with the latter being more general and flexible, for geometric correction or registration. These estimators have good capability in correcting errors contained in the RCPs, and in propagating appropriately errors of the RCPs to the corrected image with and without prior information. The objective of the CALS and our proposed RCALS estimators is to improve the accuracy of measurement value by weakening the measurement errors. The validity of the CALS and RCALS estimators are first demonstrated by applying them to perform geometric corrections of controlled simulated images. The conceptual arguments are further substantiated by a real-life example. Compared to the OLS estimator, the CALS and RCALS estimators give a superior overall performances in estimating the regression coefficients and variance of measurement errors.

Keywords: error propagation, geometric correction, ordinary least squares, registration, relaxed consistent adjusted least squares, remote sensing images.

1 Introduction

Remote Sensing technologies have been widely applied to monitor natural and man-made phenomena such as desertification, land cover changes, coastal environments and environmental pollutions (Chen and Tong, 1998). However, remote sensing devices have limitations such as the restrictions on spatial, spectral, temporal, and radiometric resolutions. Furthermore, the data acquisition process is affected by factors such as rotation of the earth, finite scan rate of some sensors, curvature of the earth, non-ideal sensor, variation in platform altitude, attitude, velocity and etc. (Richards and Jia, 1999). Errors corrupting the data acquisition process may be associated with both the attribute value and locations of the attribute values. Therefore, it is necessary to remove as least some of these errors prior to analysis (Jensen, 1996; Richards and Jia, 1999; Townshend, et al., 1992). One important preprocessing is geometric correction (image to map) or registration (image to image) of remotely sensed data.

The purpose of geometric correction or registration is to explicitly determine the mapping polynomials by the use of reference control points (RCPs) and then determine the pixel brightness value in the image (Jensen, 1996, Richards and Jia, 1999). The method of ordinary least squares (OLS) is most frequently used in this preprocessing. If accurate registration between images is not achieved, then spurious differences will be detected (Townshend, et al., 1992). That is, instead of comparing properties of the same location in different images, we might mistakenly compare properties of different locations instead. Accuracy of the corrected image, of course, will have direct impact on

the results of classification, change detection and data fusion.

In registration or geometric correction, the main uncertainties affecting their accuracy include (1) quality of the uncorrected or corrupted image; (2) size and arrangement of RCPs; (3) proficiency of the operator; (4) error from the model of geometric correction and (5) error from the RCPs. The effects of the first four factors on image classification and change detection have been studied in the literature (Congalton and Green, 1999; Janssen and Van der Wel, 1994; Dai and Khorram, 1998; Flusser and Suk, 1994; Moreno and Melia, 1993; Shin, 1997). Though error of the RCPs, i.e. factor 5, is one of the main sources affecting the accuracy of geometric correction for uncorrected image (as depicted in Figure 4), it has seldom been studied (Congalton and Green, 1999; Townshend et al., 1992; Carmel et al, 2001; Dai and Khorram, 1998). Since RCPs mainly come from GIS and remote sensing images, errors in the RCPs are essentially due to errors in data processing and data analysis (Lunetta, et al., 1991). Such errors will then be propagated to the corrected image during the process of registration or geometric correction.

Though the most effective way to improve the accuracy of geometric correction is through ground survey with differential GPS, it is generally too costly for implementation. Statistical procedures, such as regression are usually employed as a surrogate. In this context, common questions for registration or geometric correction are: (1) When the reference control points contain errors, how would these errors affect the regression coefficients and the accuracy of registration? (2) How large an error in the explanatory

variables is negligible? (3) How to correct the errors contianed in the explanatory variables in order to improve the accuracy of registration? (4) Most importantly, how to propagate errors in the RCPs to the corrected image and measure it accordingly? Since the OLS estimator of the regression coefficients is biased when the explanatory variables have errors (see section 2.2 for details), registration based on OLS does not appropriately propagate errors from the RCPs to the corrected image. Though researchers such as Buiten (1988, 1993) employed a variance-ratio and data-snooping test for the residuals calculated in the registration, error propagation and compensation of errors in the RCPs have not been discussed. It is well known that error propagation plays a crucial role in the uncertainty about remotely sensed images and the RCPs, as explanatory variables in the regression equation, always contain errors. Therefore, it is essential to develop new feasible methods to handle such a problem.

In this paper, we only concentrate on error analysis in image-to-image registration. We introduce the consistent adjusted least squares (CALS) estimator and propose a relaxed consistent adjusted least squares (RCALS) method for registration. These estimators have good capability in correcting errors contained in the RCPs, and to propagate correctly errors of the RCPs to the corrected image with and without prior information. The objective of the CALS and our proposed RCALS estimators is to improve the accuracy of measurement value by weakening the measurement errors.

We first introduce OLS and CALS in Section 2 and then propose RCALS for better performance. In section 3, we employ the CALS and RCALS estimators to perform the

registration of simulated images, and compare the results with OLS. A real-life example is then used to further substantiate the conceptual arguments in section 4. We then conclude our paper with a summary and viewpoint in section 5.

2 The Regression Model and Estimation Methods

In this section, we first introduce a multiple linear measurement error (ME) model, also called errors-in-variables model in statistics, in which both the response variable and explanatory variables contain measurement errors. Limitations of the classical estimation method, i.e. the OLS method, are identified. Then, a flexible approach, the CALS, is introduced as a more appropriate method to handle errors in variables. The RCALS, which can overcome the shortcomings of CALS, is then proposed for more flexible applications. Finally, we examine the issue of error propagation and give a significance test.

2.1 Multiple Linear ME Model

In statistics, the standard multiple linear ME model assumes that the "true" response h and "true" explanatory vector $\mathbf{?}$ are related by

$$h = b_0 + \mathbf{?}^{\mathrm{T}} \mathbf{ß} . \tag{1}$$

Due to measurement errors, we can only observe variables y and $\mathbf{x}$. That is,

$$\begin{aligned} y &= h + e, \\ \mathbf{x} &= \mathbf{?} + \mathbf{d}, \end{aligned} \tag{2}$$

where the observed variables are $\mathbf{x}$ and y; the unobserved true variables are $\mathbf{?}$ and h,

and the measurement errors are $\boldsymbol{d}$ and e.

As always been done, with $\hat{b}_0 = \bar{h} - \bar{\boldsymbol{?}}^{\mathrm{T}} \hat{\boldsymbol{ß}}$, equation (1) becomes $\hat{h} - \bar{h} = (\boldsymbol{?} - \bar{\boldsymbol{?}})^{\mathrm{T}} \hat{\boldsymbol{ß}}$. To facilitate our discussion, we assume in this paper that all data are centered. Thus, for a sample of size n, equations (1) and (2) become

$$\begin{aligned} \mathbf{Y} &= \boldsymbol{?}\ \boldsymbol{ß} + \mathbf{e}, \\ \mathbf{X} &= \boldsymbol{?} + \mathbf{D}. \end{aligned} \tag{3}$$

Let

$$\mathbf{Y} \equiv \begin{pmatrix} y_1 \\ \vdots \\ y_n \end{pmatrix},\ \boldsymbol{?} \equiv \begin{pmatrix} \boldsymbol{?}_1^{\mathrm{T}} \\ \vdots \\ \boldsymbol{?}_n^{\mathrm{T}} \end{pmatrix},\ \mathbf{e} \equiv \begin{pmatrix} e_1 \\ \vdots \\ e_n \end{pmatrix},\ \mathbf{X} \equiv \begin{pmatrix} \mathbf{x}_1^{\mathrm{T}} \\ \vdots \\ \mathbf{x}_n^{\mathrm{T}} \end{pmatrix},\ \mathbf{D} \equiv \begin{pmatrix} \mathbf{d}_1^{\mathrm{T}} \\ \vdots \\ \mathbf{d}_n^{\mathrm{T}} \end{pmatrix},$$

where $\mathbf{x}_i \in R^p$, $\boldsymbol{ß} = (b_1, \cdots, b_p)^{\mathrm{T}}$, $\boldsymbol{?}_i$ and $\mathbf{d}_i$ are p-dimensional vectors, while h_i, y_i, and e_i are scalars. The measurement errors $(\mathbf{d}_i^{\mathrm{T}}, e_i)$ are independent identically distributed (i.i.d.) random vectors, which are independent of the true values $\boldsymbol{?}_i$.

2.2 OLS Estimator

If we ignore the measurement error when regressing $\mathbf{Y}$ on $\mathbf{X}$, the OLS estimators of $\boldsymbol{ß}$ and s_e^2 are respectively

$$\hat{\boldsymbol{ß}}_{OLS} = (\mathbf{X}^{\mathrm{T}}\mathbf{X})^{-1}\mathbf{X}^{\mathrm{T}}\mathbf{Y}, \tag{4}$$

$$(\hat{s}_e^2)_{OLS} = \tfrac{1}{n-p}\mathbf{Y}^{\mathrm{T}}[\mathbf{I}_n - \mathbf{X}(\mathbf{X}^{\mathrm{T}}\mathbf{X})^{-1}\mathbf{X}^{\mathrm{T}}]\mathbf{Y}. \tag{5}$$

It should be noted that the above two expressions are no longer consistent estimators of $\boldsymbol{ß}$ and s_e^2 (Wansbeek and Meijer, 2000). In fact,

$$\mathbf{Y} = \boldsymbol{?}\ \boldsymbol{ß} + \mathbf{e} = \mathbf{X}\boldsymbol{ß} + \tilde{\mathbf{e}}, \quad \text{where } \tilde{\mathbf{e}} = \mathbf{e} - \mathbf{D}\boldsymbol{ß}. \tag{6}$$

$\tilde{\mathbf{e}}$ shares a stochastic term $\mathbf{D}$ with the regressor matrix $\mathbf{X}$ (see (3)). It implies that $\tilde{\mathbf{e}}$ is

correlated with $\mathbf{X}$ and hence $E(\tilde{\mathbf{e}} \mid \mathbf{X}) \neq \mathbf{0}$. This lack of orthogonality means that a crucial assumption underlying the use of OLS is violated.

2.3 CALS Estimator

We consider the case that there is a sufficient number of restrictions on the parameters for model identification. These restrictions can be combined with the statistics from OLS to yield a consistent estimator of the model parameters. This estimation method is called consistent adjusted least squares (CALS) (Kapteyn and Wansbeek, 1984; Wansbeek and Meijer, 2000).

We now consider equation (3). Assume that rows of $\mathbf{D}$ are i.i.d. with zero expectation and covariance matrix $\mathbf{S}_D$, and are uncorrelated with $\mathbf{?}$ and $\mathbf{e}$, i.e., $E(\mathbf{D} \mid \mathbf{?}) = \mathbf{0}$ and $E(\mathbf{e} \mid \mathbf{D}) = \mathbf{0}$. Let $\mathbf{S}_\Xi \equiv \frac{1}{n}\mathbf{?}^{\mathrm{T}}\mathbf{?} \xrightarrow{P} \mathbf{S}_\Xi$, then $\mathbf{S}_X \equiv \frac{1}{n}\mathbf{X}^{\mathrm{T}}\mathbf{X} \xrightarrow{P} \mathbf{S}_X$. It can be shown (Wansbeek and Meijer, 2000) that

$$\hat{\mathbf{ß}}_{OLS} = (\mathbf{X}^{\mathrm{T}}\mathbf{X})^{-1}\mathbf{X}^{\mathrm{T}}\mathbf{Y} \xrightarrow{P} \mathbf{ß} - \mathbf{S}_X^{-1}\mathbf{S}_D\mathbf{ß} = (\mathbf{I} - \mathbf{S}_X^{-1}\mathbf{S}_D)\mathbf{ß}. \tag{7}$$

The bias of the OLS estimator of $\mathbf{ß}$ is

$$w \equiv -\mathbf{S}_x^{-1}\mathbf{S}_D\mathbf{ß}. \tag{8}$$

When there is no measurement error, $\mathbf{S}_D = \mathbf{0}$, it implies that $w = 0$ and OLS is consistent. In addition,

$$(\hat{s}_e^2)_{OLS} = \frac{1}{n-p}\mathbf{Y}^{\mathrm{T}}[\mathbf{I}_n - \mathbf{X}(\mathbf{X}^{\mathrm{T}}\mathbf{X})^{-1}\mathbf{X}^{\mathrm{T}}]\mathbf{Y} \xrightarrow{P} s_e^2 + \mathbf{ß}^{\mathrm{T}}\mathbf{S}_D\mathbf{S}_X^{-1}\mathbf{S}_\Xi\mathbf{ß} \geq s_e^2 \tag{9}$$

can be obtained.

◆ ***Prior Information Known***

If $\mathbf{S}_D$ were known we can obtain a least squares estimator that is adjusted to attain consistency, denoted by CALS1 (Here CALS1 is used to distinguish it from the CALS estimator without prior information, which is denoted by CALS2)

$$\hat{\boldsymbol{ß}}_{CALS1} = (\mathbf{I} - \mathbf{S}_X^{-1}\mathbf{S}_D)^{-1}\hat{\boldsymbol{ß}}_{OLS} \xrightarrow{P} \boldsymbol{ß} \qquad \text{(from (7))} \tag{10}$$

or

$$\hat{\boldsymbol{ß}}_{CALS1} = (\mathbf{S}_X - \mathbf{S}_D)^{-1}\mathbf{S}_{XY} \xrightarrow{P} \boldsymbol{ß}\ , \tag{11}$$

where $\mathbf{S}_{XY} \equiv \frac{1}{n}\mathbf{X}^{\mathrm{T}}\mathbf{Y}$. Thus, the CALS estimator $\hat{\boldsymbol{ß}}_{CALS1}$ can obtain better regression results than OLS when there are measurement errors in variables.

◆ ***Prior Information Unknown***

In practice, $\mathbf{S}_D$ is rarely known. We adopt the following equation to estimate the regression coefficients, denoted by CALS2.

$$\hat{\boldsymbol{ß}}_{CALS2} = (\mathbf{I} - \mathbf{S}_X^{-1}\hat{l})^{-1}\hat{\boldsymbol{ß}}_{OLS}\ , \tag{12}$$

if $\mathbf{S}_D = s_e^2\mathbf{I}$, where $\hat{l}$ is the minimum eigenvalue of S, i.e. the minimum solution of $|\mathbf{S} - l\ \mathbf{I}| = 0$ and $\mathbf{S}$ is defined as

$$\mathbf{S} \equiv \begin{pmatrix} \mathbf{Y}^{\mathrm{T}}\mathbf{Y} & \mathbf{Y}^{\mathrm{T}}\mathbf{X} \\ \mathbf{X}^{\mathrm{T}}\mathbf{Y} & \mathbf{X}^{\mathrm{T}}\mathbf{X} \end{pmatrix}. \tag{13}$$

As an illustration, we simulate one set of data (listed in Table 1) to compare the performances of equations (4), (10) and (12). In this experiment, we give the true value of regression coefficients $\boldsymbol{ß} = (ß_0, ß_1, ß_2)^{\mathrm{T}} = (1,\ 2,\ 3)^{\mathrm{T}}$ and the true value of $\mathbf{S}_D = \begin{pmatrix} 1.0 & 0.5 \\ 0.5 & 1.0 \end{pmatrix}$.

The objective of this experiment is to investigate the performances of OLS, CALS1, CALS2. $\hat{b}_i, i = 0, 1, 2$ are the estimators of regression coefficients.

From Table 2, we can observe that the estimator of CALS2 obviously outperforms the others. However, equation (12) is obtained under the assumption that $\mathbf{S}_D = s_e^2\mathbf{I}$. This assumption is restrictive in many practical applications. In order to overcome this disadvantage, a new estimator, called the relaxed CALS (denoted as RCALS), is proposed in the following subsection.

2.4 The Relaxed CALS (RCALS) Estimator

We relax the assumption $\mathbf{S}_D = s_e^2\mathbf{I}$ into a more general relationship: $\mathbf{S}_D = t\,\mathbf{I}$, where $t > 0$ is scalar. That is, s_e^2 and t are not necessary equal to each other. According to the definition of $\mathbf{S}_D$, $\mathbf{S}_D = t\,\mathbf{I}$ implies that all errors in the explanatory variables are independent and have the same variance t. It should be noted that the CALS estimator of ß is

$$\begin{aligned}\hat{\boldsymbol{ß}}(t) &= \hat{\boldsymbol{ß}}_{CALS} \\ &= (\mathbf{I} - \mathbf{S}_X^{-1}\mathbf{O}_D)^{-1}\hat{\boldsymbol{ß}}_{OLS} \\ &= (\mathbf{S}_X - t\,\mathbf{I})^{-1}\mathbf{S}_X(\mathbf{S}_X^{-1}\mathbf{S}_{XY}) \\ &= (\mathbf{S}_X - t\,\mathbf{I})^{-1}\mathbf{S}_{XY}.\end{aligned} \tag{14}$$

When t is very small, (14) can be expressed approximatively as

$$\hat{\boldsymbol{ß}}(t) = (\mathbf{S}_X^{-1} + t\,\mathbf{I})\,\mathbf{S}_{XY}. \tag{15}$$

According to the idea of orthogonal regression, we can establish the objective function $f(t)$ as follows:

$$f(t) = \frac{(\mathbf{Y}\text{-}\mathbf{X}\hat{\boldsymbol{ß}}(t))^{\mathrm{T}}(\mathbf{Y}\text{-}\mathbf{X}\hat{\boldsymbol{ß}}(t))}{1+\hat{\boldsymbol{ß}}(t)^{\mathrm{T}}\hat{\boldsymbol{ß}}(t)}. \tag{16}$$

We thus select t, as the estimator of variance s_d^2 of all explanatory variables, such

that $f(t)$ is minimized. The optimization problem reduces to the solution of the following quadratic equation

$$a_0 + a_1 t + a_2 t^2 = 0 \ , \tag{17}$$

where

$$\begin{aligned}
&a_0 \equiv -2C_0\mathbf{a}^{\mathrm{T}}\mathbf{b} - C_1\mathbf{a}^{\mathrm{T}}\mathbf{a}, \\
&a_1 \equiv 2C_0\mathbf{b}^{\mathrm{T}}\mathbf{b} - 2C_2\mathbf{a}^{\mathrm{T}}\mathbf{a}, \\
&a_2 \equiv C_1\mathbf{b}^{\mathrm{T}}\mathbf{b} + 2C_2\mathbf{a}^{\mathrm{T}}\mathbf{b}, \\
&\mathbf{a} \equiv \mathbf{Y} - \mathbf{X}\hat{\boldsymbol{ß}}_{OLS}, \\
&\mathbf{b} \equiv \mathbf{X}\mathbf{S}_{XY} \ , \\
&C_0 \equiv 1 + \mathbf{S}_{XY}^{\mathrm{T}}\mathbf{S}_X^{-2}\mathbf{S}_{XY}, \\
&C_1 \equiv 2\mathbf{S}_{XY}^{\mathrm{T}}\mathbf{S}_X^{-1}\mathbf{S}_{XY}, \\
&C_2 \equiv \mathbf{S}_{XY}^{\mathrm{T}}\mathbf{S}_{XY} \ .
\end{aligned} \tag{18}$$

It can be shown that a solution to equation (17) is positive and the other is negative. Only the positive solution $\hat{t}$ can be selected as the estimator of s_d^2. Thus we have

$$\begin{cases}
\hat{s}_d^2 = \hat{t} \ , \\
\hat{s}_e^2 = \frac{1}{n}(\mathbf{Y} - \mathbf{X}\hat{\boldsymbol{ß}}_{OLS})^{\mathrm{T}}(\mathbf{Y} - \mathbf{X}\hat{\boldsymbol{ß}}_{OLS}) - \hat{t}\,\hat{\boldsymbol{ß}}_{LS}^{T}(\mathbf{I} - \hat{t}\mathbf{S}_X^{-1})^{-1}\hat{\boldsymbol{ß}}_{OLS} \ , \\
\hat{\boldsymbol{ß}} = (\mathbf{I} - \hat{t}\,\mathbf{S}_X^{-1})^{-1}\hat{\boldsymbol{ß}}_{OLS} \ .
\end{cases} \tag{19}$$

2.5 The Error Propagation Model

One of the great advantages of the CALS and the proposed RCALS estimators over OLS is that they can propagate errors. Having an error propagation mechanism is crucial to the analysis of remotely sensed data. Now we can rewrite the variance estimators of measurement errors of the explanatory variables and response variables for these estimators as follows:

$$\text{OLS:} \quad \hat{s}_e^2 = \frac{1}{n-p}\mathbf{Y}^{\mathrm{T}}[\mathbf{I}_n - \mathbf{X}(\mathbf{X}^{\mathrm{T}}\mathbf{X})^{-1}\mathbf{X}^{\mathrm{T}}]\mathbf{Y} . \tag{20}$$

$$\text{CALS: } \hat{s}_e^2 = \begin{cases} \hat{s}_d^2 = \hat{l}\,, & \text{if } \mathbf{S}_D = s_e^2\mathbf{I} \\ (\hat{s}_e^2)_{OLS} - \hat{\boldsymbol{\beta}}_{OLS}^{\mathrm{T}}\mathbf{S}_D\hat{\boldsymbol{\beta}}_{OLS}\,, & \text{if } \mathbf{S}_D \text{ is konwn} \end{cases}. \tag{21}$$

$$\text{RCALS: } \begin{cases} \hat{s}_d^2 = \hat{t} \\ \hat{s}_e^2 = \frac{1}{n}(\mathbf{Y} - \mathbf{X}\hat{\boldsymbol{\beta}}_{OLS})^{\mathrm{T}}(\mathbf{Y} - \mathbf{X}\hat{\boldsymbol{\beta}}_{OLS}) - \hat{t}\,\hat{\boldsymbol{\beta}}_{OLS}^{\mathrm{T}}(\mathbf{I} - \hat{t}\,\mathbf{S}_X^{-1})^{-1}\hat{\boldsymbol{\beta}}_{OLS}\,, \\ \text{if } \mathbf{S}_D = t\,\mathbf{I}\,. \end{cases} \tag{22}$$

From equations (21) and (22), we can know that CALS and RCALS estimators can obtain the variance estimators of measurement errors and propagate the errors in the explanatory variables to the response variable according to the law of error propagation from equations (1) and (2). OLS, on the other hand, does not have such a capability. Subsequently, we can obtain the estimator of variance of the response variable as follows:

$$\begin{aligned} s_y^2 &= \boldsymbol{\beta}^{\mathrm{T}}\mathbf{S}_{\Xi}\boldsymbol{\beta} + s_e^2 \\ &= \boldsymbol{\beta}^{\mathrm{T}}\mathbf{S}_X\boldsymbol{\beta} - \boldsymbol{\beta}^{\mathrm{T}}\mathbf{S}_D\boldsymbol{\beta} + s_e^2\,, \end{aligned} \tag{23}$$

where $\mathbf{S}_X$ is the variance matrix of the measurement vector of $\mathbf{X}$.

Here, we have two situations:

(a) When **?** is a deterministic variable, we can obtain the variance estimator of the response variable as

$$\hat{s}_y^2 = \hat{s}_e^2\,. \tag{24}$$

(b) When **?** is a random variable, the variance estimator of the response variable is obtained as

$$\hat{s}_y^2 = \hat{\boldsymbol{\beta}}^T(\mathbf{S}_X - \hat{\mathbf{S}}_D)\hat{\boldsymbol{\beta}} + \hat{s}_e^2\,. \tag{25}$$

2.6 The Significance Test

We answer here the question on how small an error in the explanatory variables can

we ignore. In other words, we need to have a significance test on the variances of the measurement errors.

Under the assumptions: $\mathbf{S}_D = s_e^2\mathbf{I}$ and $s_d^2 = s_e^2 = s^2$, it can be proved that the approximate relationship $\hat{s}_e^2 \sim N(s^2, 2s^4)$ holds (Kapteyn and Wansbeek, 1984). In order to test whether s^2 differs significantly from zero, we first specify a sufficiently small positive $s_0^2 > 0$. The one-side significance test is structured as follows:

$$\mathbf{H}_0 : s^2 \le s_0^2 \quad \longleftrightarrow \quad \mathbf{H}_1 : s^2 > s_0^2$$

When the inequality $\hat{s}_e^2 \ge (1+\sqrt{2}U_a)s_0^2$ holds (where U_a is the a upper quantile of the standard normal distribution), $\mathbf{H}_0$ is rejected at the significance level a. We can say that there are significant measurement errors in the regression variables under the assumption $\mathbf{S}_D = s_e^2\mathbf{I}$.

3 Empirical Analysis in the Registration of Simulated Images

In the remaining part of this paper, we discuss how to apply CALS and RCALS estimators to improve the accuracy in registering simulated images and remotely sensed data. For validating the CALS and RCALS estimator, we first employ some simulation studies to examine the characteristics and effects of RCPs with errors on the accuracy of registration in this section. We then apply the method to a real-life remotely sensed image in the next section.

Registration generally includes two procedures: (a) a registration being a geometric rearrangement of the pixels; (b) a resampling of the pixel values on the basis of the new

pixel arrangement (Buiten and Clevers, 1993). Procedure (a) mainly consists of two methods: interpolation and trend function. Interpolation is a mathematical treatment of the transformation and is totally dependent on the control points. Trend function is more or less a statistical approach to the adjustment of the residuals of the control points by OLS.

After the geometric rearrangement of two "images" has been performed in procedure (a), a resampling of the pixel values will be made on the basis of the new pixel arrangement. Procedure (b) mainly consists of nearest neighbour resampling, bilinear interpolation or cubic convolution. In this paper, we adopt the interpolation method and neighbour resampling.

3.1 Mapping registration into Polynomials

It is assumed that a map (or an image) corresponding to the concerned image is of higher level of accuracy geometrically. Location of a point on the map is defined by coordinates (g_x, g_y) and that of the image is defined by coordinates (m_x, m_y). Suppose that the two coordinate systems can be related via a pair of mapping functions f and h so that

$$\begin{cases} m_x = f(g_x, g_y), \\ m_y = h(g_x, g_y) \ . \end{cases} \tag{26}$$

Though explicit forms for the mapping functions in equation (26) are not known, they are generally chosen as simple polynomials of first, second or third degree. For example, in the case of first order polynomial, the pair functions are expressed as

$$\begin{cases} z_1 = m_x = b_{01} + b_{11}g_x + b_{21}g_y , \\ z_2 = m_y = b_{02} + b_{12}g_x + b_{22}g_y . \end{cases} \tag{27}$$

Let $\mathbf{?} = (g_x,\ g_y)^{\mathrm{T}}$ and $\mathbf{ß}_{(i)} = (b_{1i},\ b_{2i})^{\mathrm{T}}$, $i = 1,\ 2$. Then equation (27) can be written as

$$\begin{cases} z_1 = b_{01} + \mathbf{?}^{\mathrm{T}}\mathbf{ß}_{(1)} , \\ z_2 = b_{02} + \mathbf{?}^{\mathrm{T}}\mathbf{ß}_{(2)} . \end{cases} \tag{28}$$

For the case of second order polynomial, the pair functions are

$$\begin{cases} z_1 = m_x = b_{01} + b_{11}g_x + b_{21}g_y + b_{31}g_x g_y + b_{41}g_x^2 + b_{51}g_y^2 , \\ z_2 = m_y = b_{02} + b_{12}g_x + b_{22}g_y + b_{32}g_x g_y + b_{42}g_x^2 + b_{52}g_y^2 . \end{cases} \tag{29}$$

If we let $\mathbf{?} = (g_x,\ g_y,\ g_x g_y,\ g_x^2,\ g_y^2)^{\mathrm{T}}$ and $\mathbf{ß}_{(i)} = (b_{1i},\ b_{2i}, ..., b_{5i})^{\mathrm{T}}$, $i = 1,\ 2$, then the above equations can still be expressed into (28).

Thus, based on the OLS, CALS, RCALS estimators discussed above, we can obtain the corresponding estimators of the regression coefficients and variance estimators of the measurement errors.

3.2 Simulation Study

The approach taken in this paper combines formal mathematical modeling with simulation and is based on an error with specified properties (Arbia, et al., 1999). The simulation study uses artificially generated images with specified image properties. The purpose of using images and errors with simple but well defined properties is to better understand the characteristics and effects of CALS and RCALS estimators on the improvement of accuracy of geometry correction in a controlled environment. The problem with using real images (rather than artificially generated images) is that real

images usually have complex structures and real errors are usually not known. Thus it becomes difficult to evaluate the effectiveness of using CALS and RCALS in image registration.

3.2.1 Simulated data

◆ ***Simulated ideal image***

To reduce matching error during the process of collecting pairs of control points, we simulate one black and white image. The simulated ideal image is also called the master image. We used the Arc/Info Grid module, Arc Macro language and IDL programming language for this simulation. A 512-by-512 thematic raster simulated image was constructed, with one of the K classes assigned randomly to each pixel, according to predetermined class proportions. Here, we define k =2, that is, two classes, and the class proportion is 1:1. Pixels of the first class were given 50 in gray value and the left were given 240 in gray value in order to enhance the contrast (Figure 1).

◆ ***Corrupted Simulated Image***

Corrupted Simulated Image is also called slave image or uncorrected image. The goal to simulate the error and add the error in the ideal image is to validate the CALS and RCALS estimators. The corrupting process can include different types of transformations, such as translation, scale, rotation, skewing and random position error. Mathematically, the transformation can be simulated via equation (29).

To avoid the effect of resampling and interpolation on image registration (Dai and

Khorram, 1998) and to facilitate our comparing the corrected result and the simulated ideal image, we artificially create the corrupted image from the simulated ideal image. First, we translate the simulated ideal image in the *x* and *y* directions by 2 pixels respectively. Second, we add random positional error with 2-pixels variance into that image to obtain the corrupted image. Though the simulated corrupted image is not as complicated as the real corrupted image, this simplification, without loss of generality, does not affect our analysis. It should be noted that the error of each pixel is introduced through the same mechanism with a 2-pixels variance, so all pixels in the corrupted image are with variance 2 (Figure 2).

3.2.2 Matching Images

As mentioned above, registration includes two procedures, namely interpolation and neighbour resampling. Here we mainly discuss the interpolation method, i.e. the regression model.

◆ ***Collecting Control Points***

The first step to registration is to collect control points in a map or a reference image. This is a very important process to improve the accuracy of registration. Accurate identification of control points is a prerequisite for obtaining an accurate registration (Janssen and Van der Wel, 1994). A sufficient number of well defined control-point pairs must be chosen to rectify an image to ensure that accurate mapping polynomials can be generated. However, attention must also be given to the locations of the points. A general

rule is that there should be a distribution of control points around the edges of the image to be corrected with a scattering of points over the body of the image. This is to ensure that the mapping polynomials are well-behaved over the image (Richards and Jia, 1999). The sample of control points is subjected to uniform distribution, so the regression model belongs to structure regression model (Wansbeek and Meijer, 2000). In this simulation study, matching error of the locations of the points is controlled within 0.1 pixels. Figure 3 shows the distribution of control points in the simulated ideal image. Table 3 shows the control points in the simulated ideal image.

◆ ***Adding Random Error into Reference Control Points***

In collecting the control points, we limit the matching error of their locations within a very small neighborhood so that the impact of matching error on the accuracy of the registration can be ignored. These control points are then taken as the ideal reference control points, i.e. error free. When the RCPs are error free, the regression coefficients of the CALS and RCALS are same as that of the OLS (see section 2 for details). In order to test the ability of the CALS and RCALS in rectifying a deviation, we artificially add random errors into the RCPs. The range of the variance of errors is from 0.1 to 4.0. In this way, we can observe systematically and quantitatively the impact of errors in the RCPs on the accuracy of the registration. We performed 20 simulated experiments and averaged the 20 realizations to form the relationship between error in the control points and accuracy of the regression coefficients (Figure 4). When we add just a 0.5-pixel variance to the RCPs, the corrected image obtained by the OLS estimator differs significantly from

the simulated ideal image (Figure 5). That is, the registered quality is greatly lowered under small errors in the RCPs.

◆ ***Registration***

Before calculating the regression coefficients using the CALS and RCALS estimators, control points from the master image and slave image should be centralized as:

$$\begin{cases} \mathbf{x}_{center} = \mathbf{x} - \bar{\mathbf{x}} \\ \mathbf{y}_{center} = \mathbf{y} - \bar{\mathbf{y}} \end{cases}, \tag{30}$$

We then put $\mathbf{x}_{center}$ and $\mathbf{y}_{center}$ into the CALS, RCALS and OLS estimators respectively. To avoid the impact of resampling and interpolation on the registration, the slave image is produced by one order deformation. So, we select the first order polynomial as the regression function.

In the next section, we analyze the results of the registration based on the CALS, RCALS and OLS estimators.

3.3 Analysis Results and Interpretation

3.3.1 The Comparision of Estimators

In this paper, we adopt two methods to compare the performances of the estimators: namely the mean square error (MSE), commonly used in regression analysis, and the difference between the reference and corrected images. Here we use the difference image to analyze the effect of CALS, RCALS and OLS estimators. Accordingly, we make use of

the mean and standard deviation of the difference images to depict the difference between the results obtained by the CALS, RCALS and OLS methods.

◆ ***The comparision of regression coefficients***

Here, we adopt the MSE of the regression coefficient estimators to analyze their effects on the accuracy of image registration. The method is detailed as follows:

Let

$$R = \mathrm{MSE}(\hat{\boldsymbol{\beta}}) = E(\hat{\boldsymbol{\beta}} - \boldsymbol{\beta})^{\mathrm{T}}(\hat{\boldsymbol{\beta}} - \boldsymbol{\beta}). \tag{31}$$

The estimator of MSE is

$$\hat{R} = \frac{1}{k}\sum_{i=1}^{k}(\hat{\boldsymbol{\beta}}^{(k)} - \overline{\boldsymbol{\beta}})^{\mathrm{T}}(\hat{\boldsymbol{\beta}}^{(k)} - \overline{\boldsymbol{\beta}}), \tag{32}$$

where k is the number of samples, $\hat{\boldsymbol{\beta}}^{(k)}$ is the estimator corresponding to the kth sample and $\overline{\boldsymbol{\beta}}$ is the mean of $\hat{\boldsymbol{\beta}}^{(k)}$, $i = 1, ..., k$.

We tested the 20 simulation experiments for different s_d^2 and the same $s_e^2 = 2$ and tabulate three of these experiments as representatives in Table 4, i.e. s_d^2 = 1, 2 and 2.5; $s_e^2 = 2$; $\tilde{\boldsymbol{\beta}}_{(1)} = (b_{01}, \boldsymbol{\beta}_{(1)}^{\mathrm{T}})^{\mathrm{T}} = (b_{01}, b_{11}, b_{21})^{\mathrm{T}} = (2,0,1)^{\mathrm{T}}$, $\tilde{\boldsymbol{\beta}}_{(2)} = (b_{02}, \boldsymbol{\beta}_{(2)}^{\mathrm{T}})^{\mathrm{T}} = (b_{02}, b_{12}, b_{22})^{\mathrm{T}} = (2,1,0)^{\mathrm{T}}$ in (27) and $\mathbf{S}_D = s_d^2\mathbf{I}$. We also calculate the $\hat{R}$ value under different values of s_d^2, and find that CALS2 have better performance than the others.

We can make several observations from Table 4. First, CALS2 sometimes give good estimation of the regression coefficients. For example, the $\hat{R}$ value is the smallest when s_d^2 = 2 and 2.5, but it is the largest when s_d^2 = 1. The reason is that CALS2 is effective for large samples from the statistics point of view. However, it is well known that collecting sample points is time-consuming and expensive. So, the sample size must be kept to a

minimum (Lunetta, 1991). That is, the sample size may not always meet the qualification of large samples. Consequently, the experimental results obtained by CALS2 are not always consistent with the theoretical result. Second, CALS and RCALS estimators give superior overall performances in estimating the regression coefficients and variance of measurement error. Third, we can observe that the variance estimators of the measurement error of the output variable of CALS2 are the smallest among these variance estimators. The reason is that CALS2 utilizes more information than the others (see Equation (21)).

◆ ***Image Difference***

After a corrupted simulated image is corrected, the difference between the corrected image and the ideal image is small. So, under this condition, image difference is an effective and simple method to analyze the effect on registration based on CALS, RCALS and OLS estimators.

Image differencing generally involves the subtraction of different images. The subtraction results in positive and negative values in areas of change and zero values in areas of no change (Jensen, 1996). Since the simulated image is an 8-bit image, pixel values range from 0 to 255 and the potential range is from –255 to 255. The results are normally transformed into positive values by adding a constant, c. The operation is expressed mathematically as

$$\Delta s_{ijk} = CI_{ijk}(1) - RI_{ijk}(2) + c \tag{33}$$

where Δs_{ijk} = change in pixel value, $CI_{ijk}(1)$ = brightness value at time 1, $RI_{ijk}(2)$ =

brightness value at time 2, c = constant. $i = 1,....,$ number of lines, $j = 1,....,$ number of columns, $k =$ band k.

When obtaining the difference image, we use the mean and standard deviation to compare the results of CALS2 and OLS. In PCI software, we use histogram analysis to obtain the mean and standard deviation of the difference images. The mean and standard deviation obtained by CALS2 are 9.529 and 46.86 respectively, and that of OLS are 9.690 and 47.23 respectively. Figures 6-9 depict the result of the registration. Table 5 shows that CALS2 has better performance than OLS.

3.3.2 The Error Propagation of Remotely Sensed Data

Basic statistics about an original include the mean, standard deviation and degree of autocorrelation. It is essential to know how these statistics will change in the corrected image and how the errors of the control points will propagate. We have produced in subsection 3.2.1 a simulated ideal image free of errors. The corrupted image is produced by translating the simulated ideal image in the x and y directions by 2 pixels and by adding random positional error with a 2-pixel variance. We can regard the corrupted simulated image as the original image that was obtained with kinds of system errors and random errors by remote sensors. After the corrupted image has been registered, called the rectified image or corrected image, we have a corresponding change in uncertainty. Through equations (21) and (22), we can obtain the variance estimator of the measurement errors s_e^2 and s_d^2. From equation (24), we can derive the variance of each

pixel of the rectified image after registration $\hat{s}_y^2 = \hat{s}_e^2$. It should be noted that the true values of RCPs are deterministic variables, not random variables. In Table 4, we can find the estimators of CALS2 CALS1 and RCALS. Therefore, we need to perform statistical test to see if the errors are significant.

3.3.3 The Significance Test

A common belief is that when errors in variables are small at some significance level they can be ignored. We consider the following null and alternative hypotheses:

$$\mathbf{H}_0 : \ s^2 \le s_0^2 \quad \longleftrightarrow \quad \mathbf{H}_1 : \ s^2 > s_0^2$$

Choose $s_0^2 = 0.1$ and $a = 0.05$, we then obtain

$$\hat{s}_e^2 \ge (1+\sqrt{2}U_a)s_0^2 = 0.33. \ (\text{as } U_a = 1.645)$$

For the first group of data in Table 4, we find $\hat{s}_e^2 = 0.60237374$ and 0.44582912 respectively. Thus we reject $\mathbf{H}_0$. That is, s^2 is more than s_0^2 at 0.05 level of significance.

3.3.4 Evaluation and comparison of Estimators

Basing on the analysis and discussion in the above sections, we summarize the characteristics of CALS and RCALS when applied to image registration as follows: the models have good ability to (1) correct the error contained in RCPs (as detailed in section 2); (2) estimate correctly the error of RCPs to uncorrected image with and without prior information (as detailed in sub sections 3.1-3.3); (3) compensate the model errors, specifically improving the accuracy of $\hat{ß}$, and consequently the accuracy of the model; (4)

estimate the propagated error in the rectified image (as detailed in sub sections 3.1-3.3).

The above are the common properties of CALS and RCALS. There are however some differences between CALS and RCALS. As aforementioned, CALS is implemented under the assumption that $\mathbf{S}_D = s_e^2\mathbf{I}$, i.e. $s_e^2 = s_d^2$. This assumption is too restrictive in many practical applications. To overcome this disadvantage, RCALS is formulated by relaxing the assumption $\mathbf{S}_D = s_e^2\mathbf{I}$ into a more general relationship: $\mathbf{S}_D = s_e^2\mathbf{I}$. That is, s_e^2 and s_d^2 are not necessarily equal to each other. And, it has been argued that RCALS can better estimate the variance of the measurement errors.

Though CALS and RCALS possess the above advantages when errors exist in the variables, there are some problems that need to be further examined:

(1) From the point of view of statistics, the models are effective under large sample theory. For small sample, though the result of regression is sometimes not very good, better result should be obtained if the methods can be used in the whole process of the registration or other relevant processes in handling remotely sensed data.

(2) The models can be made more perfect when the order of regression is high. It is because the models have good compensation ability to linear regression.

(3) The arrangement of control points can affect the result of regression based on CALS and RCALS. The variation in the accuracy of registration should be investigated with reference to the variation of control-point arrangement.

4 The Registration of Remotely Sensed Data

To illustrate the applicability of the proposed estimator, we applied our methods to the study of a real-life SPOT multispectral image acquired over Xinjiang, China on August 30, 1986. The size of the data set is 3000-by-3000 pixels with three channels. A 800-by-818 subset of the source image is used in this experiment (Figure 10). The RCPs are obtained from ETM multispectral image acquired on September 30, 2000. The matching error of the locations of the points should be controlled within 0.1 pixels, so that the impact of matching error on the accuracy of the registration can be ignored.

In this example, we do not have any prior information, i.e. s_e^2 and s_d^2 are unknown. What we have done is to use the ME models to estimate the variance of the measurement errors of the explanatory variables and response variables from the sample data. For CALS estimator, the prerequisite for estimating the variance of the measurement errors is $s_e^2 = s_d^2$ when prior information is unknown. However, it is not practical in the registration of remotely sensed data. General speaking, the value of s_e^2 is much larger than that of s_d^2. So under this condition, RCALS estimator is suitable.

Before the registration of a remote sensing image, some preprocessings need be done. For efficient computation, we first convert the Geodetic Coordinates of RCPs RG ($RG = (RG_x\ RG_y)^{\mathrm{T}}$) into the corresponding image coordinates RI ($RI = (RI_x\ RI_y)^{\mathrm{T}}$). The RCPs are shown in Table 6. RI ($RG_{\min} = (RG_{\min x}\ RG_{\min y})^T$) means the minimum vector in the x direction and y direction.

$$\begin{cases} RI_x = (RG_x - RG_{\min x})/20, \\ RI_y = (RG_y - RG_{\min y})/20. \end{cases} \tag{34}$$

And then these control points are put into the OLS and RCALS estimators. Table 7 and Figure 11-12 show the result of the registration. At the same time, we can obtain variances of the measurement errors. We can observe from Table 7 that in a noisy environment the RCALS estimator has an overall superior performance compared to OLS.

5 Conclusion

We have discussed some basic issue of error analysis in image-to-image registration, and have proposed an errors-in-variables model, called RCALS, for registration. It has been demonstrated that the OLS model is incapable of handling problems in which errors exist in the response and explanatory variables. While CALS is a suitable model to perform the task, it is too restrictive in its assumption. By introducing a more general relationship, the proposed RCALS model is more flexible in analyzing errors in registration. It also renders significance test and error propagation mechanism. The conceptual arguments have been substantiated by some simulated and real-life experiments.

While the proposed RCALS model has a reasonably good performance, there are issues that need further investigations. In this paper, we have discussed the registration of corrupted image with the same error variance. For better application, we need to examine the registration of corrupted image with different error variance and with certain degree

of autocorrelation in further studies. To be more comprehensive, detailed analysis should be made on the impact of RCPs with error on the accuracy of change detection and data fusion of multi-spectral and multi-temporal remotely sensed data. Based on the proposed error propagation method, we should also discuss the impact of RCPs on the accuracy of classification of remotely sensed data. Furthermore, the error propagation of radiometric correction and its impact on the accuracy of classification should also be carried out in the future.

Reference

[1] Arbia, G.; Griffith, D.; Haining, R., 1999, error propagation modeling in raster GIS: adding and ratioing operations, *Cartography and Geographic Information Science*, Vol. 26(4), pp.297-315.

[2] Boggs, P.T.; Donaldson, J.R.; Schnabel, R.B. and Spiegelman, C.H., 1988, A computational examination of orthogonal distance regression. *Journal of Econometrics*, Vol. 38, pp.169-201.

[3] Buiten, H. J., 1988, Matching and mapping of remote sensing images: aspects of methodology and quality. *Proceedings of 16th ISPRS congress*, Kyoto, Japan, 27-B10 (III), pp. 321-330.

[4] Buiten, H. J.; Clevers, J. G. P. W., 1993, *Land observation by remote sensing: theory and applications*, Gordon and Breach Science Publisher, USA.

[5] Carmel, Y.; Dean, D. J.; Flather, C. H., 2001, Combing location and classification error sources for estimating multi-temporal database accuracy, *Photogrammetic Engineering and Remote Sensing*, Vol. 67(7), pp. 865-872.

[6] Chen, S. P.; Tong, Q. X., 1998, *The mechanism research of Remote Sensing Information*, China: Science Press.

[7] Congalton, R. G.; Green, K., 1999, *Assessing the Accuracy of Remotely Sensed Data: Principle and Practices*, Lewis Publishers.

[8] Dai, X. L.; Khorram, S., 1998, The effects of image misregistration on the accuracy of remotely sensed change detection. *IEEE Transactions on Geoscience and Remote Sensing*, Vol. 36(5), pp.1566-1577.

[9] Flusser, J.; Suk, T., 1994, A moment-based approach to registration of images with affine geometric distortion, *IEEE Transactions on Geoscience and Remote Sensing*, Vol. 32(2), pp.382 –387.

[10] Heuvelink, G. B. M., 1998, *Error propagation in environmental modelling with GIS*, London; Bristol, PA: Taylor & Francis.

[11] Itten, K. I.; Meyer, P., 1993, Geometric and radiometric correction of TM data of mountainous forested areas, *IEEE Transactions on Geoscience and Remote Sensing*, Vol. 31(4), pp.764 –770.

[12] Janssen, L. L. F.; Van der Wel, F. J. M., 1994, Accuracy Assessment of Satellite Derived Land-Cover Data: A Review, *Photogrammetic Engineering and Remote Sensing*, Vol. 60(4), pp.419-426.

[13] Jensen, J. R., 1996, *Introductory digital image processing: a remote sensing perspective*, Upper Saddle River, N.J.: Prentice Hall.

[14] Kapteyn, A.; Wansbeek, T.J., 1984, Errors in variables: Consistent Adjusted Least Squares (CALS) estimator. *Communication in Statistics ----Theory and Methods*, 13, 1811-1837.

[15] Lunetta, R. S.; Congalton, R. G.; Fenstermaker, L. K., et al., 1991, Remote Sensing and Geographic Information System Data Integration: Error Sources and Research Issues, *Photogrammetic Engineering and Remote Sensing*, 57(6): 677-687.

[16] Moreno, J. F.; Melia, J., 1993, A method for accurate geometric correction of NOAA AVHRR HRPT data, *IEEE Transactions on Geoscience and Remote Sensing*, Vol. 31(1), pp.204 –226.

[17] Nyquist, H., 1988, Least orthogonal absolute deviations. *Computational Statistics*

& Data Analysis, Vol. 6(4), pp. 361-367.

[18] Pal, M., 1980, Consistent moment estimators of regression coefficients in the presence of errors in variables. *Journal of Econometrics*, Vol. 14(2), 349-364.

[19] Richards, J. A.; Jia, X. P., 1999, *Remote sensing digital image analysis: an introduction*, Berlin; New York: Springer-Verlag, 3rd ed.

[20] Seto, Y.; Homma, K.; Komura, F., 1991, Geometric correction algorithms for satellite imagery using a bi-directional scanning sensor, *IEEE Transactions on Geoscience and Remote Sensing*, Vol. 29(2), pp.292 –299.

[21] Shin, D.; Pollard, J.K.; Muller, J. P., 1997, Accurate geometric correction of ATSR images, *IEEE Transactions on Geoscience and Remote Sensing*, Vol. 35(4), pp.997-1006.

[22] Townshend, J. R.; Justice, C. O., 1992, The Impact of Misregistration on Change Detection, *IEEE Transactions on Geoscience and remote sensing*, Vol. 30(5), pp.1054-1060.

[23] Wansbeek, T.; Meijer, E., 2000, *Measurement error and latent variables in econometrics*, Amsterdam; New York: Elsevier.

Figures:

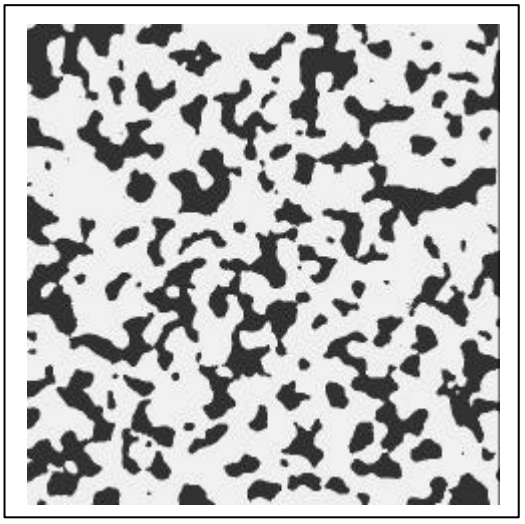

Fig.1 A Simulated Ideal Image. The size is 512-by-512

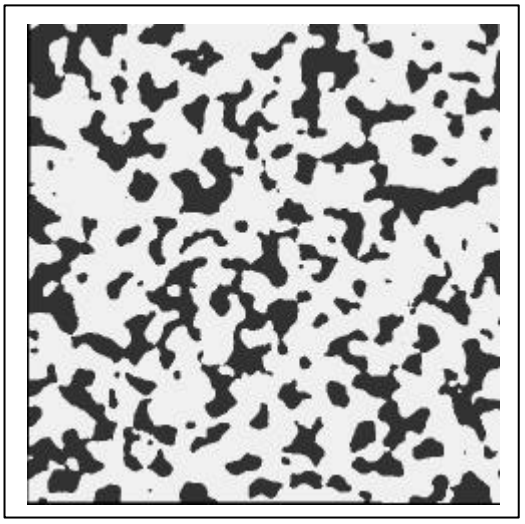

Fig. 2 The Corrupted Simulated Image

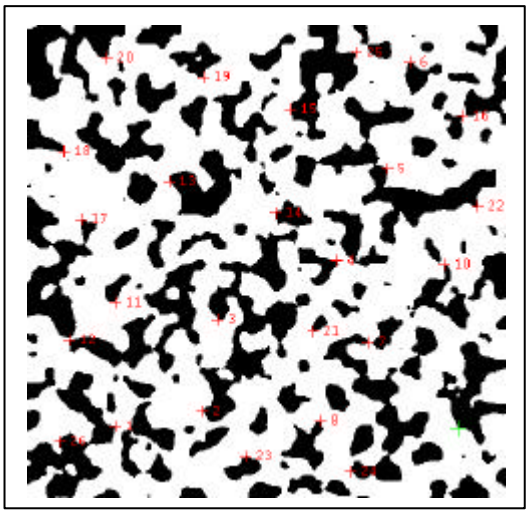

Fig. 3 The Distribution of Control Points in the Simulated Ideal Image

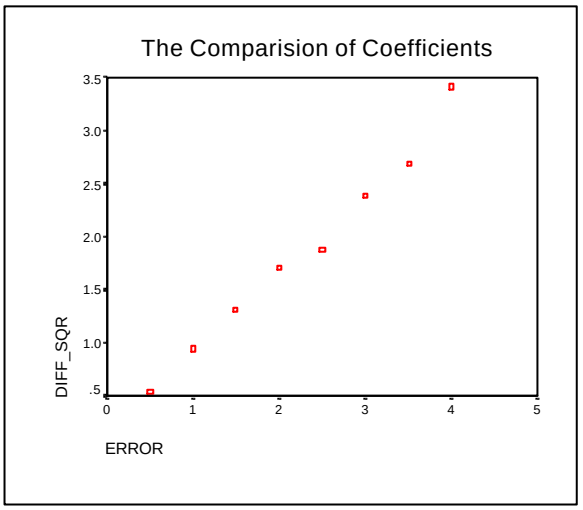

Fig. 4 The Effect of Reference Control Points (RCP) with Errors on Registration

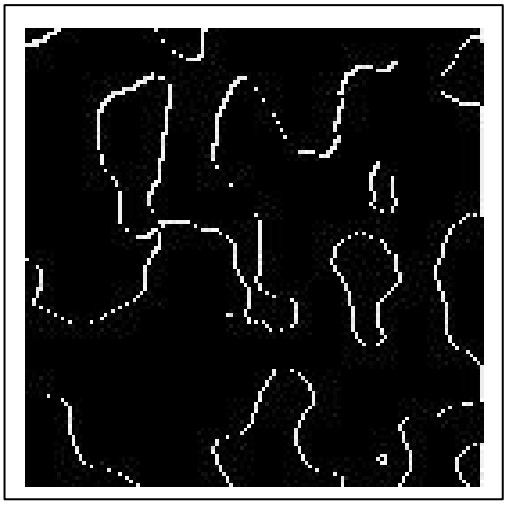

Fig. 5 The Difference Image between the Corrected Image and the Simulated Ideal Image
(RCP with 0.5-pixel variance; the corrected image is obtained by the OLS. The size of this image is 128-by-128)

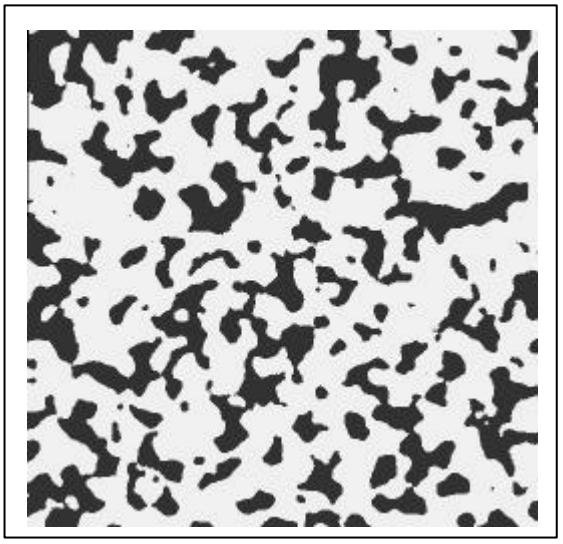

Fig. 6 Corrected Image by CALS2

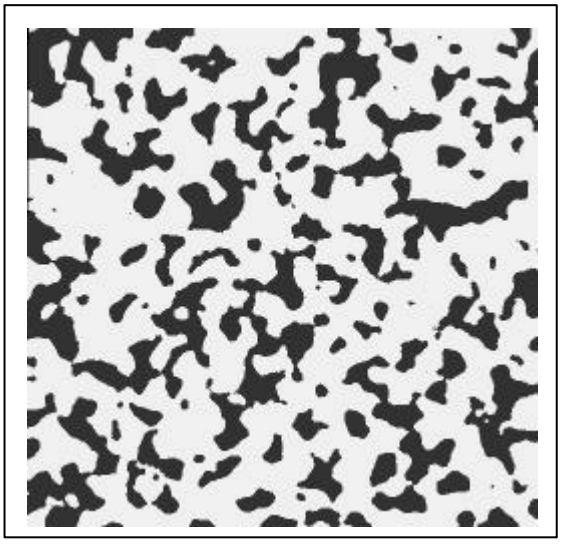

Fig.7 Corrected Image by OLS

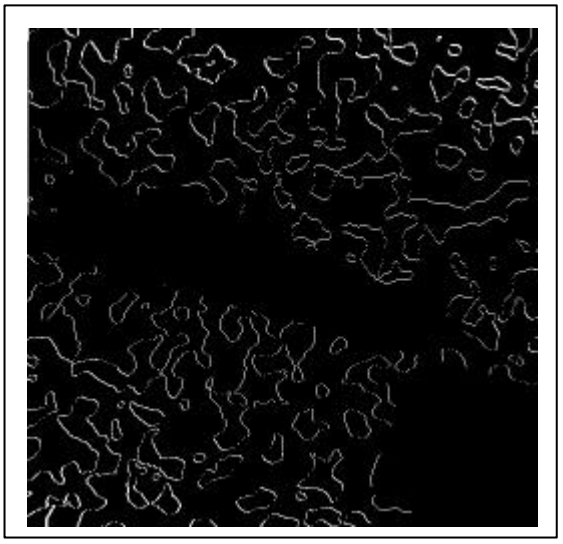

Fig. 8 Difference Image between the Corrected Image
by CALS2 and the Simulated Ideal image

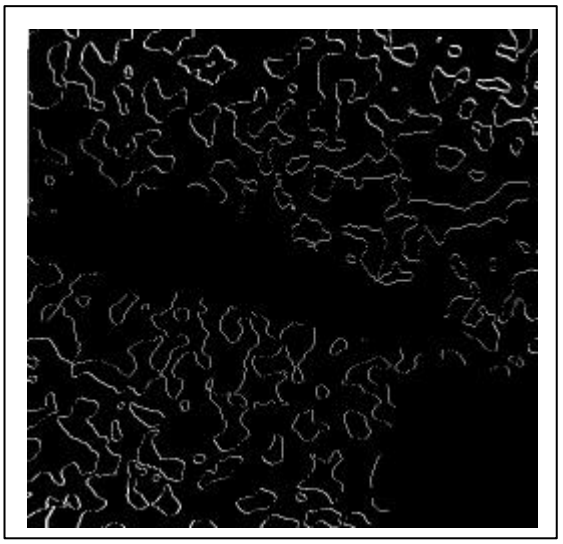

Fig. 9 Difference Image between the Corrected Image by OLS and the Simulated Ideal image

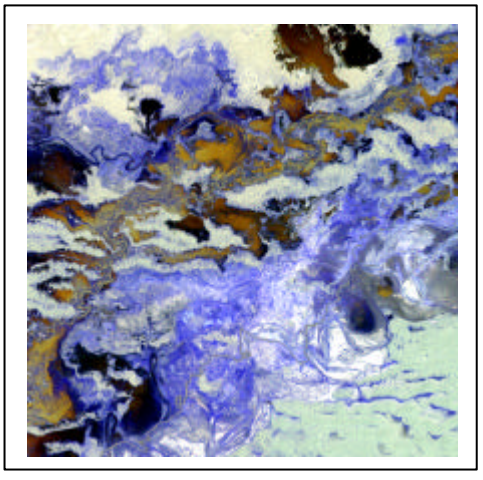

Fig. 10 SPOT Multispectral image acquired over Xinjiang on August 30, 1986

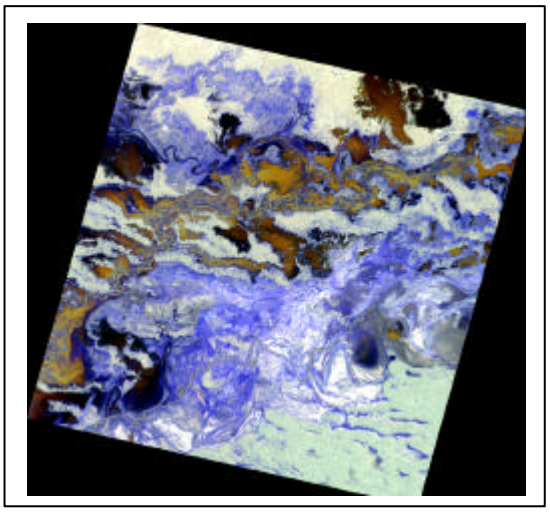

Fig. 11 Corrected Image by RCALS

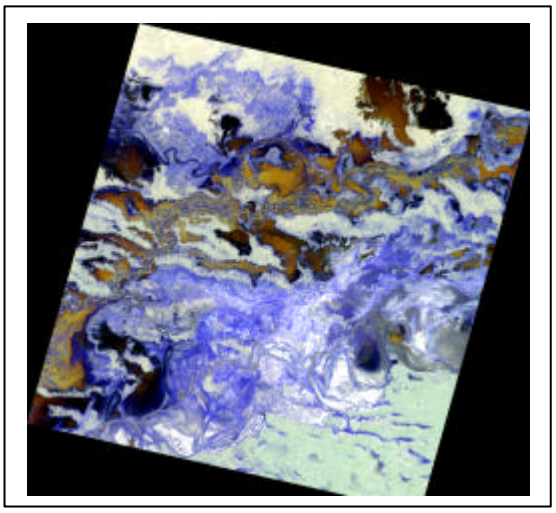

Fig. 12 Corrected Image by OLS

Tables:

Table 1 A simulated data set of size 35 (XI, YI are the explanatory variables; XO is the response variable)

XI	YI	XO	XI	YI	XO	XI	YI	XO
-1.09	-1.89	-4.7	4.13	0.05	12.79	2.78	1.1	2.42
-0.25	1.2	4.78	2.46	4	17.67	-0.1	1.84	6.62
-1.06	-2.46	-7.36	2.87	1.19	5.78	-1.74	-2.35	-11.76
1.24	-2.94	0.64	2.04	0.85	0.63	-1.34	-0.01	2.14
-1	-2.76	-8.13	1.44	0.72	5.21	-0.81	-1.86	-9.67
-4.37	-0.28	-9.34	2.27	0.6	7.15	1.21	1.58	7.39
-2.47	-2.98	-5.56	-6.53	-2.51	-16.83	2.59	3.68	15.88
-0.51	0.5	7.95	-0.21	1.98	2.26	0.18	0.51	2.97
-0.64	0.77	-3.55	-2.21	-0.91	-2.56	1.08	3.64	12.32
1.55	-0.71	0.72	-2.15	-0.44	-3.45	-3.15	-2.94	-10.63
-0.57	1.38	3.24	3.74	2.41	17.96	2.26	4.52	14.36
-1.19	-1.08	-2.81	-1.78	-0.54	0.27			

Table 2 The estimation results

	$\hat{b}_0$	$\hat{b}_1$	$\hat{b}_2$
True	1	2	3
OLS	1.247	1.806	2.313
CALS1	1.128	1.717	3.006
CALS2	1.119	2.042	3.132

Table 3 A sample of simulated data with size 24

(g_x, g_y are explanatory variables; m_x, m_y are response variables.)

g_x	g_y	m_x	m_y	g_x	g_y	m_x	m_y
95.99609	426.0039	93.99609	426.0039	266.0039	199.0039	264.0039	198.9961
188.9961	410.0039	186.9961	410.0039	281.9961	90.00391	280.0039	90.00391
204.9961	312.9961	202.9961	312.9961	465.0039	97.00391	463.0039	97.00391
331.9961	250.0039	329.9961	250.0039	60.00391	206.0039	58.00391	206.0039
384.9961	152.0039	383.0039	152.0039	41.99609	133.9961	39.00391	133.9961
408.9946	39.00391	407.0039	39.00391	190.9844	54.98438	188.0039	55.00391
364.9972	337.0039	362.9961	337.0039	88.00391	34.99609	84.99609	34.99609
314.0039	420.0039	312.0039	420.0039	306.9961	325.0039	305.0039	325.0039
446.0039	254.0039	444.0039	254.0039	481.9961	192.0039	479.9961	192.0039
95.99219	294.0078	93.99609	294.0039	234.0039	458.0039	232.0039	458.0039
47.00391	334.0039	45.00391	334.0039	347.0039	474.0039	345.0039	474.0039
152.9961	166.0039	151.0039	165.9961	351.9961	29.00391	350.0039	29.00391

Table 4 The Comparision of Regression Coefficients

($\hat{R}$ is the estimator of MSE; $\tilde{\boldsymbol{\beta}}_{(i)}=(b_{0i}, b_{1i}, b_{2i})^{\mathrm{T}}$, $i=1, 2$, $\hat{b}_{ki}$ (k = 0, 1, 2) is the estimator of regression coefficients; $\hat{s}_e^2$ and $\hat{s}_d^2$ are the estimators of measurement errors of response variable and explanatory variables respectively.)

TRUE	Methods	$\hat{b}_{0i}$	$\hat{b}_{1i}$	$\hat{b}_{2i}$	$\hat{s}_e^2$	$\hat{s}_d^2$	$\hat{R}$
$s_e^2=2$; $s_d^2=1$ $\tilde{\boldsymbol{\beta}}_{(1)}=(2,0,1)^{\mathrm{T}}$ $\tilde{\boldsymbol{\beta}}_{(2)}=(2,1,0)^{\mathrm{T}}$	RCALS	2.1020844	4.1112e-007	0.99985776	1.0346276	0.17000723	0.37252052
		1.6417400	1.0002787	0.00012789653	0.77747503	0.11437380	
	CALS2	2.0918853	-4.6593e-006	0.99990336	0.31434077	1	0.38087295
		1.6303770	1.0003250	0.00012249023	0.027603082	1	
	CALS1	2.0967715	-2.2301e-006	0.99988151	0.60237374	0.60237374	0.37520691
		1.6374874	1.0002961	0.00012587328	0.44582912	0.44582912	
	OLS	2.1041733	1.4496e-006	0.99984843	1.3140926		0.37168957
		1.6432074	1.0002728	0.00012859465	0.97299483		
$s_e^2=2$; $s_d^2=2$ $\tilde{\boldsymbol{\beta}}_{(1)}=(2,0,1)^{\mathrm{T}}$ $\tilde{\boldsymbol{\beta}}_{(2)}=(2,1,0)^{\mathrm{T}}$	RCALS	2.6537296	0.001143149	0.99665739	1.0090178	0.16381646	0.741790
		2.3505358	1.0003343	-0.0012377029	2.2830002	0.33580188	
	CALS2	2.6313630	0.001132091	0.99675731	0.70857441	2	0.712061
		2.3292396	1.0004213	-0.0012479744	0.85563459	2	
	CALS1	2.6485651	0.001140596	0.99668046	0.58782690	0.58782690	0.731403
		2.3380819	1.0003852	0.0012437094	1.3090501	1.3090501	
	OLS	2.6557249	0.001144135	0.99664848	1.2782615		0.745584
		2.3548326	1.0003168	-0.0012356308	2.8571141		
$s_e^2=2$; $s_d^2=2.5$ $\tilde{\boldsymbol{\beta}}_{(1)}=(2,0,1)^{\mathrm{T}}$ $\tilde{\boldsymbol{\beta}}_{(2)}=(2,1,0)^{\mathrm{T}}$	RCALS	1.4577786	0.000206181	1.0016535	2.5736210	0.42452286	1.626953
		3.5339340	0.99776894	-0.0033031654	2.4216008	0.35231270	
	CALS2	1.4321678	0.000193157	1.0017682	0.76372139	2.5	1.610265
		3.5068180	0.99788040	-0.0033170057	0.53525467	2.5	
	CALS1	1.4445419	0.00019945	1.0017128	1.4972648	1.4972648	1.619109
		3.5208429	0.99782275	-0.0033098468	1.3892341	1.3892341	
	OLS	1.4630165	0.00020884	1.0016300	3.2722243		1.629413

Table 5 The Comparision of Difference Image

True	Methods	$\hat{b}_{0i}$	$\hat{b}_{1i}$	$\hat{b}_{2i}$	$\hat{R}$	Mean	Standard Deviation
$s_e^2=2;$ $s_d^2=3$	CALS2	3.3501924	-0.0048645	0.99895008	2.3689419	9.529	46.86
		3.9464883	0.9955764	-0.00231508			
	OLS	3.4107636	-0.0048309	0.99867598	2.4548868	9.690	47.23
		4.0090204	0.9953184	-0.00228226			

Table 6 A sample of remotely sensed data with size 24; UI(X), UI(Y) are explanatory variables; RI(X), RI(Y) are output variables. UI means Uncorrected Image; RI means Reference Image

UI (X)	UI (Y)	RI (X)	RI (Y)	UI (X)	UI (Y)	RI (X)	RI (Y)
286.0625	711.8125	387911.2545	4546732.804	665.9688	503.9688	396411.5670	4549062.491
223.8125	789.9375	386272.5046	4545495.304	336.1875	615.0625	389396.2546	4548375.304
197.9375	254.9375	388668.7546	4555901.554	331.9688	811.9062	388253.4421	4544590.616
672.0625	572.9375	396146.2545	4547711.554	321.0625	647.4375	388938.7546	4547797.804
616.0625	392.0625	396030.0045	4551454.054	273.0625	797.0625	387202.5045	4545131.554
538.8750	231.8750	395407.5045	4554866.554	651.9375	600.9375	395602.5046	4547257.804
507.0312	626.0312	392665.3170	4547410.616	158.9094	451.4419	386864.7046	4552304.317
452.0625	698.0625	391196.2546	4546271.554	174.9961	120.0039	388964.7827	4558604.552
392.0625	269.4375	392368.1295	4554778.429	683.9961	78.0117	399064.7046	4557184.317
416.9688	404.0312	392125.3170	4552088.741	169.0039	700.0039	385704.7046	4547464.473
563.8125	688.8125	393416.2545	4545945.304	754.0039	768.0039	396684.7046	4543604.317
622.0625	638.9375	394822.5045	4546661.554	665.9688	503.9688	396411.5670	4549062.491

Table 7 The Comparision of RCALS and OLS

Methods	$\hat{b}_{0i}$	$\hat{b}_{1i}$	$\hat{b}_{2i}$	$\hat{s}_e^2$	$\hat{s}_d^2$
RCALS	47.881707	0.27295907	0.96943027	0.022603986	0.55769935
	-170.90637	0.97551516	0.22110812	0.012265135	0.54363945
OLS	47.881935	0.27295885	0.96942965	0.63592436	
	-170.90626	0.97551490	0.22110810	0.60885484	